CHAPTER 1

INTRODUCTION

1.1 GENERAL

Surface free energies and its components between two interacting surfaces are critically important in a number of industrial applications including adhesion, coating operations, printing, deinking, lubrication; and has an influence in daily life, biology, chemistry and biochemistry (1-5). Many of the mineral processing techniques, e.g. flotation, selective flocculation, filtration, thickening also depend on the interfacial interactions between solid and liquid, essentially water. These interactions are mainly controlled by the interfacial tension between two phases, which dictates the strength of interaction. The characterization of the surface properties and especially the surface free energy components of the solids are, therefore, recognized as the key to understanding the mechanism of surface-based phenomena. This information provides essential insight into the mechanism of such interactions as the stability of colloidal suspensions, molecular self-assembly, wetting, spreading, bubble-particle, particle-particle interaction in the industrial applications.

Contact angle measurements, first described by Thomas Young in 1805, remains at present the simplest and most accurate method for characterizing the surface properties of solids and determining the interaction energy between a liquid (L) and a solid (S), at the minimum equilibrium distance (6-11). The value of contact angle θ is a measure of the competing tendencies between the energy of cohesion of the liquid molecules and the energy of adhesion between liquid and solid. When the work of cohesion between liquid molecules exceeds the work of adhesion between solid and liquid, a drop of liquid placed onto the solid surface forms a finite contact angle. On the contrary, if the work of adhesion is higher than the work of cohesion spreading occurs. The water contact angle is more often used as a measure of surface hydrophobicity (12-16), i.e., the higher the contact angle is, the more hydrophobic the solid surface becomes. It can also be used to calculate the surface free energy of a solid surface. In principle, solids having lower surface free energies (γ_S) exhibit higher values of water contact angles (17-20).

The contact angle measurements are easy to perform on a smooth and flat surface, and there are several well-known techniques for measuring the contact angles of liquids on flat surfaces. By placing a drop of water on the surface of a solid of interest, the contact angle can easily be measured through the aqueous phase at the three-phase contact, i.e., solid-liquid-air. To prepare a smooth flat surface, a mineral specimen is cut by a diamond saw and polished with an abrasive powder such as alumina. It is well known, however, that mineral surfaces, particularly those of sulfide minerals, undergo significant chemical changes and atomic rearrangements during polishing. Therefore, it would be more desirable to measure contact angles directly on powdered samples. It is also unreliable and impractical to use the conventional contact angle measurement techniques for the characterization of fine powders such as fillers, pigments and fibers.

Some times the solids of interest exist only in powdered form, in which case the sessile drop technique cannot be used for contact angle measurements. It becomes somehow difficult to obtain the value of contact angle, when the solid is in powdered form. Despite the difficulties associated with the contact angle measurements, some methods are available for determining the contact angles of powders (11, 21). The capillary rise (22-24) and thin layer wicking (25-26) methods are most commonly used for powdered solids.

Another method of determining the contact angles of powders is to measure the heat of immersional wetting in various testing liquids, e.g. water, formamide, etc. In this technique, a powdered sample is degassed to remove the pre-adsorbed water and then immersed in liquid (23, 27-31). In general, the more hydrophobic a solid is, the lower the heat of immersion in water becomes. Thus, one should be able to obtain the values of contact angles from the heats of immersion and converting it into the contact angle value using thermodynamic relations. Different investigators use different methods of calculating contact angles from the heat of immersion (29-31).

Besides obtaining the contact angle values of various liquids on powdered solid surfaces, microcalorimeter may be used to determine percentages of hydrophobic and hydrophilic surface, and acidic and basic surfaces of powdered solids (32-37). The interactions between various reagents and solid surfaces in aqueous or non-aqueous media can be studied by using a microcalorimeter as well (38-42). Microcalorimetric

studies should also be particularly useful in explaining the physico-chemical aspects of mineral separation techniques such as flotation, selective flocculation and coagulation.

It is the objective of the present work, in general, to characterize the solid surfaces in the powdered form in terms of their surface free energy components (the total, γ_S; the Lifshitz-van der Waals, γ_S^{LW}; the Lewis acid-base, γ_S^{AB}; the Lewis electron donor, γ_S^- and the Lewis electron acceptor, γ_S^+) and compare to those of flat surfaces. To meet this objective, a flow microcalorimeter was used to determine the heat of immersion and heat of adsorption enthalpies of various liquids on a number of powdered talc surfaces. Also, direct contact angle measurements were conducted using various liquids to determine the surface free energy parameters of talc samples. Another objective of the present work was to study the role of surface free energies and their components in mineral separation, e.g. in flotation and selective flocculation. To this end, a crude clay from east Gergia (d_{90}=2.0 μm) sample was chosen as a model ore and subjected to flotation and selective flocculation experiments to remove anatase (TiO_2), which is the main discoloring impurity found in kaolin clay. Microcalorimetric and direct contact angle measurements were conducted using anatase (TiO_2) particles with varying hydrophobicities to explore the effect of surface hydrophobicity and surface free energies of solids on the separation efficiency of flotation and selective flocculation processes.

In what follows is a review of literature presented with an aim to provide a relevant background to the research presented in this work.

1.2 LITERATURE REVIEW

1.2.1 Surface Free Energy and Acid-Base Interactions

1.2.1.1 Lifshitz-Van der Waals Interactions

The existence of a general attractive interaction between a pair of neutral atoms was first postulated by van der Waals (43-44) to explain the observed deviation of a real gas behavior from the ideal gas law (Eq. [1.1]). In spite of the qualitative character of the argument used by van der Waals in his derivation, the great success of his equation of state in explaining experimental data on the properties of gases spurred thinking on the

origin of the interatomic or intermolecular forces. Van der Waals (43-44) showed that the ideal gas law,

$$P\overline{V} = RT \qquad [1.1]$$

does not apply to the real gases or liquids due to the interatomic or intermolecular forces. In Eq. [1.1], P is the pressure, $\overline{V}$ the molar volume, R the gas constant and T the absolute temperature. These non-covalent and non-electrostatic molecular forces are referred to as van der Waals forces. Van der Waals forces play a central role in all phenomena involving intermolecular forces, for while they are not as strong as Coulombic or H-bonding interactions, they are always present.

Collectively called as the van der Waals forces, these intermolecular forces originates from: a) randomly orienting dipole-dipole (or orientation) interactions, described by Keesom (45); b) randomly orienting dipole-induced dipole (or induction) interactions, described by Debye (46); c) fluctuating dipole-induced dipole (or dispersion) interactions, described by London (47-48).

a) Keesom's dipole-dipole interactions *in vacuo*:

Keesom (45) suggested that two molecules with permanent dipole moments orient themselves in such a way as to attract each other. The interaction energy due to this orientation effect is given by:

$$V = \frac{\mu_1^2 \mu_2^2}{3(4\pi\varepsilon_0)^2 kTr^6} \qquad [1.2]$$

where V is the potential energy (J), μ_1 and μ_2 dipole moments (Cm), ε_0 dielectric permittivity *in vacuo* (8.854×10^{-12} $C^2J^{-1}m^{-1}$), k Boltzman constant (1.381×10^{-23} JK^{-1}), T absolute temperature (K) and r distance between interacting atoms or molecules (m). As shown, the Keesom's interaction energy is inversely proportional to the sixth power of the interatomic distance. Note that Keesom's interactions are identical with Coulombic

interactions between two charged bodies separated by a distance *r, in vacuo* which is given by:

$$F = \frac{q_1 q_2}{4\pi\varepsilon_0 r^2} \qquad [1.3]$$

where F is the Coulomb force, q_1 and q_2 the electrical charge (C) of two interacting bodies.

b) Debye's dipole-induced dipole interactions in vacuo:

Debye (46) proposed that the polarizability of molecules is the cause of intermolecular forces. He showed that a molecule with a permanent dipole moment polarizes a neighboring neutral molecule. The interaction between the electric field of these two different dipoles gives rise to an interaction force. The interaction energy can be calculated using

$$V = \frac{\alpha\mu^2}{(4\pi\varepsilon_0)^2 r^6} \qquad [1.4]$$

where α is polarizability ($C^2m^2J^{-1}$). Eq. [1.4] suggests that similar to the Keesom's interaction, Debye's interaction energy is inversely proportional to the sixth power of the interatomic distance.

c) London's fluctuating dipole-induced dipole interactions in vacuo:

The existence of attraction between pair of neutral molecules has led to the definition of the dispersion forces by London in 1930. London (47-48) showed that the energy of dispersion interaction between two atoms or molecules is obtained using

$$V = -\frac{3\alpha^2 h\nu}{4(4\pi\varepsilon_0)^2 r^6} \qquad [1.5]$$

in which h Plank's constant (6.626×10^{-34} Js) and v frequency of fluctuation (s^{-1}). As shown, the London's interaction energy is also inversely proportional to the sixth power of the interatomic distance.

The dispersion forces have been considered as a result of the charge fluctuations associated with the motion of electrons in their "orbitals". These charge fluctuations result in a time-dependent dipole moment. The phase difference in fluctuating dipoles leads to a mutual interaction, while the time-dependent dipole generates an instantaneous electric field which polarizes any neighboring neutral atom or molecule, inducing a dipole moment in it. As a result, a mutual instantaneous interaction is also generated. The interactions between the atoms or molecules obtained such a way causes an increase in the magnitude of the interaction force.

Of the there interactions given, Keesom and Debye interactions are only found among molecules which have permanent dipole moments. The Keesom theory and Debye theory in combination, therefore, have been used successfully to explain the interactions between polar molecules in a phenomenological way. On the other hand, for neutral gas molecules such as H_2, N_2 and CH_4 which posses no permanent dipole moments, the intermolecular forces deduced from Van der Waals thermal equation (Eq. [1.1]) are far greater than the force accounted for by the orientation and induction effect.

The London dispersion interaction, however, is universal and is present in atom-atom interactions as well. All three interaction energies between atoms or molecules decay very steeply with distance (r), as r^{-6}. Of the three components of intermolecular forces, only van der Waals-London (dispersion) interactions have significant importance between macroscopic bodies, in the *condensed systems* (49-50). The already small Keesom interaction is virtually completely screened out, especially in aqueous media which contain electrolytes (51). The dispersion forces play also a significant role in a number of industrially important processes such as flocculation, coagulation, adhesion, polymer conformation and physical adsorption.

I) Dispersion Forces Between Two Macroscopic Materials - Hamaker's Approach

Hamaker (52) conducted pair-wise summation of the dispersion (van der Waals-London) energies theoretically, based on microscopic interactions, for macroscopic bodies (of flat surfaces) interacting with each other.

The Hamaker constant, A_{ii}, is commonly used to estimate the dispersion interaction at short distances between two microscopic bodies of material *i* as given by:

$$A_{ii} = \pi^2 q_i^2 \beta_{ii} \qquad [1.6]$$

where q_i is the number of atoms per unit volume and β_{ii} the London constant for the interaction between two atoms *i*, i.e., $\beta_{ii} = 3\alpha^2 h\nu / 4(4\pi\varepsilon_0)^2$ (see Eq. [1.5]).

The total attractive dispersion energy, V_{London}, for two flat parallel surfaces, separated by a distance *r*, is given by:

$$V_{London} = -\frac{A_{ii}}{12\pi r^2} \qquad [1.7]$$

which allows one to determine the dispersion interaction energy between two atoms or molecules of material *i* using Hamaker's constant.

Knowing that $\beta_{ii} = 3\alpha^2 h\nu / 4(4\pi\varepsilon_0)^2$, the Eq. [1.5] can be rewritten as:

$$V = -\frac{\beta_{ii}}{r^6} \qquad [1.8]$$

which is useful for calculating dispersion interaction energy from the known value of London constant.

According to the Berthelot's principle (53), the interaction constant between two particles of different materials equals to the geometric mean of the interaction constants of individual materials. Thus, the London constant, β_{ii}, between two different types of atoms or molecules can be written as:

$$\beta_{ij} = \sqrt{\beta_{ii}\beta_{jj}} \qquad [1.9]$$

It follows that

$$A_{ij} = \sqrt{A_{ii}A_{jj}} \qquad [1.10]$$

which is known as *geometric mean combining rule (Berthelot)*, and is widely used for calculating dispersion energies of interaction between dissimilar materials.

By assuming additivity and using Hamaker's pair-wise summation it can be shown that for two identical spheres of radius *R*, the (free) energy of interaction becomes,

$$V = \Delta G = -\frac{AR}{12r} \qquad [1.11]$$

and the force between the same two spheres becomes,

$$F = \frac{AR}{12r^2} \qquad [1.12]$$

Note that the force is obtained by differentiating the energy with respect to distance, i.e., $V = \int_0^r F dr$.

For two interacting flat parallel surfaces, the attractive (dispersion) energy may be written as:

$$V = \Delta G = -\frac{A}{12\pi r^2} \qquad [1.13]$$

and:

$$F = \frac{A}{6\pi r^3} \qquad [1.14]$$

For the other geometries, the reader is referred to the references 51 (Israelachvili) and 54 (Nir).

Hamaker's pair-wise summation procedure can also be used to calculate the combined Hamaker constant of two macroscopic identical and different particles interacting in a third medium. For two identical materials (e.g. material 1) in a medium 3, the Hamaker combining rule can be described by:

$$\begin{aligned} A_{131} &= A_{11} + A_{33} - 2A_{13} \\ &= \left(\sqrt{A_{11}} - \sqrt{A_{33}}\right)^2 \end{aligned} \qquad [1.15]$$

in which A_{11} and A_{33} refer to the Hamaker constants of the solid and the medium, respectively, in vacuo.

For materials 1 and 2 in a medium 3, the Hamaker combining rule can be given by:

$$\begin{aligned} A_{132} &= A_{12} + A_{33} - A_{13} - A_{23} \\ &= \left(\sqrt{A_{11}} - \sqrt{A_{33}}\right)\left(\sqrt{A_{22}} - \sqrt{A_{33}}\right) \end{aligned} \qquad [1.16]$$

Eq. [1.15] suggests that the value of A_{131} is always positive ($A_{131}>0$). Therefore, two identical molecules or particles in medium 3 (i.e., liquid) always attract each other, although it can become zero, when $A_{11}=A_{33}$. However, A_{132} can have negative values ($A_{132}<0$), i.e., when:

$A_{11}>A_{33}>A_{22}$, and

$A_{11}<A_{33}<A_{22}$

under which conditions the dispersion interaction energy becomes repulsive, i.e., $V_{Dispersion}>0$ (55-57).

Fowkes (6) proposed a more practical approach for determining the Hamaker constant of material *i*, from the known values of γ_i^d:

$$A_{ii} = 6\pi r_{ii}^2 \gamma_i^d \qquad [1.17]$$

in which r_{ii} is the distance between interacting atoms or molecules and γ_i^d is the dispersion component of the surface free energy of the substance in question. Fowkes (6) found that the value of $6\pi r_{ii}^2$ be 1.44 x 10^{-14} cm^2 for most materials. Thus, Eq. [1.17] allows one to calculate the value of Hamaker constant of a material from the experimentally determined value of γ_i^d or vice versa. Since the use of Eq. [1.17] only requires the value of dispersion component of surface free energy of materials that can be readily obtained from simple contact angle measurements, it is convenient to use this method for practical purposes. Due to its simplicity, this method has been widely used in practice (58-62).

It can be seen from the foregoing descriptions that the Hamaker approach to dispersion interaction between two microscopic bodies has the virtue of ease of comprehension. As an approximation, it is customary to use Equation [1.10] for the calculation of A_{ij} and Equations [1.15] and [1.16] for the calculation of A_{131} and A_{132} from the known values of A_{ii} that can be obtained from Equation [1.6]. Padday and Uffindell (63) demonstrated the applicability of Hamaker approach to the n-alkanes by calculating the theoretical values of surface tensions of various n-alkanes using the following equation:

$$W_{ii} = 2\gamma_{ii} = \frac{A_{ii}}{12\pi r_{ii}^2} \qquad [1.18]$$

where r_{ii} is the separation distance between two atoms in the bulk. The calculated results have shown a good agreement with experimentally measured values of surface tension, which suggest that the intermolecular forces of n-alkane are mainly of dispersion type. It is clear that the calculated value of surface tension depends critically on the assumed value of r_{ii}.

Table 1.1 gives the values of Hamaker constants for two identical materials interacting across vacuum (or air), along with some other properties taken from the

literature (51). As shown, the Hamaker constants for n-alkanes are substantially smaller compared to those obtained for the various minerals and metals.

Table 1.2 shows the values of Hamaker constants for two different materials in another medium other than air or vacuum (51). As shown, the Hamaker constants for n-alkanes are substantially smaller compared to those obtained for the various minerals and metals. For example, the values of Hamaker constants for n-alkanes are in the range from 3.8-5.1 x 10^{-20} J, whereas it is 43 x 10^{-20} J for rutile (TiO_2). According to the Hamaker's theoretical approach, TiO_2 should collide much faster than hydrocarbon oil in water (see Equation [1.15]). Contrary to the suggestions made by Hamaker's theoretical approach, collision tendency of hydrocarbon oil droplets in water is much higher and their collision kinetics is much faster than the particles of TiO_2 and other oxide minerals and metals. Hamaker approach, like the classical DLVO theory, ignores the existence of hydrophobic interaction between the two particles of hydrophobic materials.

II) Dispersion Forces Between Two Macroscopic Materials - Lifshitz Approach

In contrast to Hamaker's approach, which started with single interatomic interactions, to arrive at the total interaction energy for macroscopic bodies by a process of summation, Lifshitz (64) has constructed a more accurate approach through a purely macroscopic framework. The problems associated with the use of summation process have been completely eliminated in this macroscopic treatment of dispersion forces. Lifshitz treated the interacting bodies as continuous media. The dispersion forces in this approach have been derived in terms of the macroscopic properties of interacting bodies, such as their dielectric constants or refractive indexes.

Lifshitz (64) calculated interaction energy using quantum mechanical and electromagnetic approach. As mentioned, this theory is for macroscopic bodies and considers the effect of the medium and the retardation effect, which caused by a finite velocity of propagation of electromagnetic fields. The basic idea lies in the fact that oscillation of electrons around a nucleus creates an oscillation of the electromagnetic field around an atom. It has been noted that this field is always present within any medium due to thermodynamic fluctuations, and it also extends to outside of the medium.

Lifshitz's theory of condensed media interactions has its origins in Maxwell's equations, where the electric and magnetic fields are subjected to fast temporal fluctuations. In order to accommodate the temporal fluctuations of the fields, Lifshitz has adopted the fluctuation theory developed by Rystov (65). The derivation of Lifshitz model is beyond the scope of this work. Therefore, only the results and its utility are presented here.

A general expression for the free energy of interaction between two flat surfaces is given by

$$\Delta G = -\frac{A}{12\pi r^2} \qquad [1.19]$$

which is of the same form of as Eq. [1.13]. The Hamaker constant, A, may be designated as A_{132} and A_{131} for the interactions between materials 1 and 2 in a medium 3 and materials 1 and 1 in a medium 3, respectively. The Lifshitz theory gives (51):

$$A_{132} = \frac{3}{4}kT\left(\frac{\varepsilon_1-\varepsilon_3}{\varepsilon_1+\varepsilon_3}\right)\left(\frac{\varepsilon_2-\varepsilon_3}{\varepsilon_2+\varepsilon_3}\right) + \frac{3h\nu_e}{8\sqrt{2}}\frac{\left(n_1^2-n_3^2\right)^{1/2}\left(n_2^2-n_3^2\right)^{1/2}}{\left(n_1^2+n_3^2\right)^{1/2}\left(n_2^2+n_3^2\right)^{1/2}\left\{\left(n_1^2+n_3^2\right)^{1/2}+\left(n_2^2+n_3^2\right)^{1/2}\right\}} \qquad [1.20]$$

and

$$A_{131} = \frac{3}{4}kT\left(\frac{\varepsilon_1-\varepsilon_3}{\varepsilon_1+\varepsilon_3}\right)^2 + \frac{3h\nu_e}{16\sqrt{2}}\frac{\left(n_1^2+n_3^2\right)^2}{\left(n_1^2-n_3^2\right)^{3/2}} \qquad [1.21]$$

where ε_1 , ε_2 and ε_3 are the dielectric constants of the three media and n_1 , n_2 and n_3 are the refractive indexes of the same. In each of Eqs. [1.20] and [1.21], the first term on the right hand side gives the *zero-frequency energy* of the van der Waals energy (which includes the Keesom and Debye interaction energies), while the latter term represents the

dispersion energy which includes London energy contribution. v_e is the absorption frequency in the UV region ($\approx 3 \times 10^{15}$ s^{-1}) (51).

Israelachvili (66) calculated the Hamaker constants of different liquids from the data of their refractive indexes using the Lifshitz macroscopic approach. The author then calculated the surface tensions of these liquids from the already estimated values of the Hamaker constants using the following equation:

$$\Delta G_{ii} = -\frac{A_{ii}}{24\pi r_0^2} \qquad [1.22]$$

where ΔG_{ii} stands for the free energy of cohesion of species i in vacuo. Since $\gamma_i = -\frac{1}{2}\Delta G_{ii}$,

$$\gamma_i = \frac{A_{ii}}{12\pi r_0^2} \qquad [1.23]$$

where γ_i is the (apolar component) of the surface tension of material i and r_0 is the separation distance between two flat parallel surfaces when they are in van der Waals contact. Note that this is the same form of Eq. [1.18] from which Padday and Uffindell (63) calculated the theoretical values of surface tensions of various n-alkanes using Hamaker approach. The value of r_0 was defined to be 0.157±0.009 nm (51).

III) Interfacial Lifshitz-Van der Waals Interactions

Good and Grifalco (67) and Fowkes (68) showed that if only dispersion interaction forces are available between two condensed phases, e.g., a solid and a liquid, the interfacial tension (γ_{12}^{LW}) is given by the following equation:

$$\begin{aligned} \gamma_{12}^{LW} &= \left(\sqrt{\gamma_1^{LW}} - \sqrt{\gamma_2^{LW}}\right)^2 \\ &= \gamma_1^{LW} + \gamma_2^{LW} - 2\sqrt{\gamma_1^{LW}\gamma_2^{LW}} \end{aligned} \qquad [1.24]$$

which is referred to as Good-Grifalco-Fowkes combining rule.

The Lifshitz-van der Waals interaction energy between materials 1 and 2 in vacuo is given by Dupre equation (21):

$$\Delta G_{12}^{LW} = \gamma_{12}^{LW} - \gamma_1^{LW} - \gamma_2^{LW} \qquad [1.25]$$

Substituting Eq. [1.24] into Eq. [1.25] one obtains,

$$\Delta G_{12}^{LW} = -2\sqrt{\gamma_1^{LW}\gamma_2^{LW}} \qquad [1.26]$$

which is a very important relation. This equation states that the atoms at an interface are pulled by those in the neighboring phase. Since the Lifshitz-van der Waals forces are universal and always available at the surface, Eq. [1.26] also suggests that the energy of interaction is negative, i.e, the interaction energy between two condensed phases is always attractive.

Similarly, the interaction energy between molecules or particles of material 1, immersed in a liquid 2 is:

$$\Delta G_{121}^{LW} = -2\gamma_{12}^{LW} \qquad [1.27]$$

and the energy of cohesion of material 1 is:

$$\Delta G_{11}^{LW} = -2\gamma_1^{LW} \qquad [1.28]$$

Also, the energy of interaction between materials 1 and 2, in a medium 3, is given by:

$$\Delta G_{132}^{LW} = \gamma_{12}^{LW} - \gamma_{13}^{LW} - \gamma_{23}^{LW} \qquad [1.29]$$

Thus, defined values of interaction energies, i.e., $\Delta G_{11}^{LW}, \Delta G_{12}^{LW}, \Delta G_{121}^{LW}, \Delta G_{132}^{LW}$, can be linked to the respective Hamaker constants as:

$$\Delta G^{LW} = -\frac{A}{12\pi r^2} \qquad [1.30]$$

which provides one to determine the Hamaker's constant and to check the correctness of Hamaker's combining rule via a surface thermodynamic approach.

1.2.1.2 Polar or Acid-Base Interactions

It has been known for many years that acid-base interactions are important in adhesion of organic substances to inorganic substrates (69-73), but the adhesion between two nonpolar substances has been described by the term "polar" for a long period of time. The reason is that intermolecular forces were studied first in dense gases, where dispersion forces (London) dipole-dipole interactions (Keesom), and dipole-induced dipole interactions (Debye) explain most of the intermolecular interactions between pairs of atoms or molecules (43-48). For many years, these intermolecular forces were used to explain the intermolecular forces between solids and liquids, even after the discovery of the hydrogen bonding and acid-base interactions.

In the last twenty years significant advances have been made in the thermodynamic treatment and interpretation of interfacial tension between two interacting surfaces, i.e., solid and liquid. It is now clear that especially in aqueous media the polar interactions are mainly governed by the interactions between hydrogen-donors and hydrogen-acceptors (or between Bronsted acids and Bronsted bases) (21, 50, 74). It is, however, preferable to extend the concept of polar interactions more widely, including hydrogen bonds, and to define them to comprise all electron-acceptor-electron-donor, or Lewis acid-base interactions, designated by superscript AB (50, 76-79).

Fowkes (28, 68, 79) proposed that the surface tension of a material *i* can be broken down into separate components originating from different kinds of intermolecular forces:

$$\gamma_i = \sum_j \gamma_i^j \qquad [1.31]$$

where j stands for different types of surface tension component, e.g., dispersion, dipolar, induction, hydrogen bonding and metallic interactions.

One may group the different types of surface tension components into apolar (nonpolar) and polar interactions. The former can be represented by the Lifshitz-van der Waals (or LW) interactions and the latter includes all others. The polar interactions are generally considered to be interactions between Lewis acids and bases on the surface. Thus, Eq. [1.31] can be rewritten:

$$\gamma_i = \gamma_i^{LW} + \gamma_i^{AB} \qquad [1.32]$$

where γ_i^{LW} and γ_i^{AB} refer to the apolar (Lifshitz-van der Waals) and polar (acid-base) components of surface tension, respectively.

Since $\Delta G_{ii} \equiv -2\gamma_i$ by definition, Eq. [1.32] can be written:

$$\Delta G = \Delta G^{LW} + \Delta G^{AB} \qquad [1.33]$$

where ΔG^{LW} is the free energy change due to Lifshitz-van der Waals interaction, and ΔG^{AB} is the same due to acid-base interactions.

The work conducted by Fowkes (50) is probably the best example for demonstrating the presence and importance of acid-base interactions between two interacting surfaces. This author determined the values of acid-base (W_{SL}^{AB}) and Lifshitz-van der Waals (W_{SL}^{LW}) components of work of adhesion for various acidic and basic liquids on polymer surfaces as a function of acidity or basicity of polymer. He showed that the contribution of acid-base (or polar) component to the work of adhesion (W_{SL}) is strictly dependent on the acidity or basicity of the solid (polymer) of interest.

For example, when studying with polyethylene (a basic polymer) which is co-polymerized with various contents of acrylic acid (an acidic monomer), he found that the acid-base contribution to the work of adhesion increased with increasing acid content of

the polymer in the case of using basic liquids such as dimethylsulfoxide, dimetylformamide and 0.1 M aqueous solution of sodium hydroxide, in the adhesion (contact angle) measurements. However, a strongly acidic liquid (35% phenol in tricresylphosphate) had nothing but dispersion force interactions with the acidic polymer; no dipole contribution to adhesion was observed.

The author obtained similar results with acidic liquids on copolymers of ethylene with varying contents of vinyl acetate, which is a basic monomer. In this case, he showed that W_{SL}^{AB} for acidic liquids (35, 48 and 72% phenol in tricresylphosphate, respectively) increased with increasing vinyl acetate content of the polymer, and, W_{SL}^{AB} for pyridine, a basic liquid, was zero; again no dipole contribution was observed. Recently, there have been numerous publications in the field of acid-base interactions either to prove (80-83) or disprove (84-86) the existence of these types of interactions between two interacting surfaces.

Van Oss et al (87) showed, based on Fowkes's acid-base interaction approach (50), that electron-acceptor (Lewis acid) and electron-donor (Lewis base) interactions are essentially asymmetrical in the sense that of a given polar substance *i* the electron-acceptor and the electron-donor parameters are usually quite different. For acid-base interactions between materials *i* and *j*,

$$\Delta G_{ij}^{AB} = -2\sqrt{\gamma_i^+ \gamma_j^-} - 2\sqrt{\gamma_i^- \gamma_j^+} \qquad [1.34]$$

and

$$\Delta G_{ii}^{AB} = -4\sqrt{\gamma_i^+ \gamma_i^-} \qquad [1.35]$$

where γ^+ is the acidic component and γ^- is the basic component of the surface tension.

Since $\Delta G_{ii} \equiv -2\gamma_i$, Eq. [1.35] becomes:

$$\gamma_i^{AB} = 2\sqrt{\gamma_i^+ \gamma_i^-} \qquad [1.36]$$

From Dupre equation, which is applicable for any type of interaction, one may define:

$$\Delta G_{12}^{AB} = \gamma_{12}^{AB} - \gamma_1^{AB} - \gamma_2^{AB} \qquad [1.37]$$

The above relation is valid irrespective of polarity or apolarity. One can rearrange Eq. [1.37] to express the interfacial tension γ_{12}^{AB} between materials 1 and 2 as:

$$\gamma_{12}^{AB} = \Delta G_{12}^{AB} + \gamma_1^{AB} + \gamma_2^{AB} \qquad [1.38]$$

Substituting this into Eq. [1.34] and [1.36] one obtains:

$$\begin{aligned} \gamma_{12}^{AB} &= 2\left(\sqrt{\gamma_1^+\gamma_1^-} + \sqrt{\gamma_2^+\gamma_2^-} - \sqrt{\gamma_1^+\gamma_2^-} - \sqrt{\gamma_1^-\gamma_2^+}\right) \\ &= 2\left(\sqrt{\gamma_1^+} - \sqrt{\gamma_2^+}\right)\left(\sqrt{\gamma_1^-} - \sqrt{\gamma_2^-}\right) \end{aligned} \qquad [1.39]$$

which is equivalent to Eq. [1.24] for Lifshitz-van der Waals (LW) interactions.

Fowkes's surface tension components approach can be applied to interfacial tensions as follows:

$$\gamma_{12} = \gamma_{12}^{LW} + \gamma_{12}^{AB} \qquad [1.40]$$

Substituting Eqs. [1.24] and [1.39] into Eq. [1.40], one obtains the total interfacial surface free energy between phases 1 and 2:

$$\begin{aligned} \gamma_{12} &= \gamma_1^{LW} + \gamma_2^{LW} - 2\sqrt{\gamma_1^{LW}\gamma_2^{LW}} + 2\left(\sqrt{\gamma_1^+\gamma_1^-} + \sqrt{\gamma_2^+\gamma_2^-} - \sqrt{\gamma_1^+\gamma_2^-} - \sqrt{\gamma_1^-\gamma_2^+}\right) \\ &= \left(\sqrt{\gamma_1^{LW}} - \sqrt{\gamma_2^{LW}}\right)^2 + 2\left(\sqrt{\gamma_1^+} - \sqrt{\gamma_2^+}\right)\left(\sqrt{\gamma_1^-} - \sqrt{\gamma_2^-}\right) \end{aligned} \qquad [1.41]$$

It should be stressed here that the apolar interactions are additive, while the acid-base interactions are not due essentially to the asymmetric properties mentioned earlier. If one of the phases does not posses the component γ^+ or γ^- the proper term concerning them disappears in Eq. [1.41]. If phase 1 (i.e., liquid) or phase 2 (i.e., solid) does not have both electron donor (γ^-) and electron acceptor (γ^+) interactions it is termed apolar surface. If the surface possesses both components γ^+ and γ^-, it is called bipolar. Lastly, if the surface has only electron donor or electron acceptor interactions, it is named monopolar surface, but neither γ^+ nor γ^- component participates in the surface tension of a liquid or a surface free energy of a solid. However, they do participate in interfacial interactions if the contacted phase exposes the complementary component γ^+ or γ^-, respectively (21). Eq. [1.41] shows that apolar (or dispersion) component is always positive, while polar (or acid-base) component can be positive or negative.

The Dupre equation can also be used in the form of:

$$\Delta G_{12} = \gamma_{12} - \gamma_1 - \gamma_2 \qquad [1.42]$$

to describe the interaction between materials 1 and 2, suspended in liquid 3 and by taking both the LW and AB into account and substituting Eqs. [1.24] and [1.39] into Eq. [1.42] one obtains,

$$\Delta G_{132} = 2\left[\begin{array}{l} \sqrt{\gamma_1^{LW}\gamma_3^{LW}} + \sqrt{\gamma_2^{LW}\gamma_3^{LW}} - \sqrt{\gamma_1^{LW}\gamma_2^{LW}} - \gamma_3^{LW} + \\ \sqrt{\gamma_3^+}\left(\sqrt{\gamma_1^-} + \sqrt{\gamma_2^-} - \sqrt{\gamma_3^-}\right) + \sqrt{\gamma_3^-}\left(\sqrt{\gamma_1^+} + \sqrt{\gamma_2^+} - \sqrt{\gamma_3^+}\right) \\ -\sqrt{\gamma_1^+\gamma_2^-} - \sqrt{\gamma_1^-\gamma_2^+} \end{array}\right] \qquad [1.43]$$

Eq. [1.43] suggests that the interaction energy between two different materials can be either negative (attractive) or positive (repulsive) depending on the surface free energy parameters of material 1 and 2 in medium 3, e.g. water.

Similarly, for describing the interaction between molecules or particles of material 1, suspended in liquid 3:

$$\Delta G_{131} = -2\gamma_{13} = -2\left(\sqrt{\gamma_1^{LW}} - \sqrt{\gamma_3^{LW}}\right)^2 - 4\left(\sqrt{\gamma_1^+\gamma_1^-} + \sqrt{\gamma_3^+\gamma_3^-} - \sqrt{\gamma_1^+\gamma_3^-} - \sqrt{\gamma_1^-\gamma_3^+}\right) \quad [1.44]$$

The hydrophobic interaction is more closely related to Eq. [1.44]. When low energy (or hydrophobic) materials interact with each other in aqueous systems (water is the medium 3), γ_{13} becomes positive and ΔG_{131} negative, giving rise to an attraction. If the polar surface free energy component of hydrophobic material is negligibly small, in this case the most important parameter in Eq. [1.44] is $-4\sqrt{\gamma_3^+\gamma_3^-}$ which represents the polar contribution to the cohesive energy of water. The value of $-4\sqrt{\gamma_3^+\gamma_3^-}$ is 102 mJ/m^2 and is present in all type of interactions. In fact, this term is the main contributor to the interfacial attractions between low-energy materials immersed in water (21, 88).

1.2.1.3 Van Oss-Chaudhury-Good Equation

According to Fowkes (28, 79, 89), the work of adhesion (W_a) between a liquid on a solid surface proposed to be given by:

$$W_a = W_{ad}^d + W_{ad}^{nd} \quad [1.45]$$

where W_a^d represents the contributions from dispersion (nonpolar) interactions, and W_a^{nd} represents the same from non dispersion (polar or ionic) interactions. Laskowski and Kitchener (90) suggested that all solids would be hydrophobic if W_{ad}^{nd}=0, i.e., if the surface is free of polar groups on which water molecules can be bonded.

Fowkes (50, 75) and van Oss et al (76-78) showed that surface free energy components of a material *i* can be given by:

$$\gamma_i = \gamma_i^{LW} + \gamma_i^{AB} \quad [1.32]$$

where γ_i^{LW} and γ_i^{AB} refer to the apolar (Lifshitz-van der Waals) and polar (acid-base) components of surface tension.

For the interactions between a solid S and a liquid L, Eq. [1.33] may be written as:

$$\Delta G_{SL} = \Delta G_{SL}^{LW} + \Delta G_{SL}^{AB} \qquad [1.46]$$

where $\Delta G_{SL}{}^{LW}$ is the free energy change due to Lifshitz-van der Waals interaction, and $\Delta G_{SL}{}^{AB}$ is the same due to acid-base interactions.

Fowkes (68) showed that

$$\Delta G_{SL}^{LW} = -2\sqrt{\gamma_S^{LW}\gamma_L^{LW}} \qquad [1.47]$$

while Van Oss et al (76-78) showed that

$$\Delta G_{SL}^{AB} = -2\sqrt{\gamma_S^{+}\gamma_L^{-}} - 2\sqrt{\gamma_S^{-}\gamma_L^{+}} \qquad [1.48]$$

Substituting these into Eq. [1.46],

$$\Delta G_{SL} = -2\sqrt{\gamma_S^{LW}\gamma_L^{LW}} - 2\sqrt{\gamma_S^{+}\gamma_L^{-}} - 2\sqrt{\gamma_S^{-}\gamma_L^{+}} \qquad [1.49]$$

Let us consider a process in which an air bubble is brought to the surface of a solid immersed in water. If the solid surface is sufficiently hydrophobic, the air bubble will stick to the surface forming an angle. The angle measured between the solid surface and the surface of the air bubbles through the aqueous phase is referred to as "contact angle". Young (91) showed that

$$\gamma_L \cos\theta = \gamma_S - \gamma_{SL} \qquad [1.50]$$

where γ_L is the surface tension of water and γ_{SL} is the interfacial tension between the solid and liquid. The changes in free energy associated with the bubble-particle adhesion is given by the following relation (92):

$$\Delta G_{SL} = \gamma_{SL} - \gamma_S - \gamma_L \qquad [1.51]$$

Combining Eqs. [1.50] and [1.51],

$$-\Delta G_{SL} = \gamma_L (1 + \cos\theta) \qquad [1.52]$$

which is known as the Young-Dupre equation.

Substituting Eq. [1.52] into Eq. [1.49], one obtains:

$$(1 + \cos\theta)\gamma_L = 2\left(\sqrt{\gamma_S^{LW}\gamma_L^{LW}} + \sqrt{\gamma_S^{+}\gamma_L^{-}} + \sqrt{\gamma_S^{-}\gamma_L^{+}}\right) \qquad [1.53]$$

which is known as the Van Oss-Chaudhury-Good (OCG) thermodynamic approach to determine the values of surface free energy components of solids. This is very useful information for characterizing a solid surface in terms of its surface free energy components, i.e., γ_S^{LW}, γ_S^{+}, and γ_S^{-}. To determine these values, it is necessary to determine contact angles of three different liquids of known properties (in terms of γ_L^{+}, γ_L^{-}, γ_L^{LW}) on the surface of the solid of interest. One can then set up three equations with three unknowns, which can be solved to obtain the values of γ_S^{LW}, γ_S^{+}, and γ_S^{-}.

If an apolar liquid is placed on the surface of a talc sample and its contact angle is measured, Eq. [1.53] can be reduced to:

$$(1 + \cos\theta)\gamma_L = 2\sqrt{\gamma_S^{LW}\gamma_L^{LW}} \qquad [1.54]$$

because γ_L^{+} and γ_L^{-} are zero. Thus, Eq. [1.54] can be used to determine γ_S^{LW} from a single contact angle value, provided that the contact angle measurement is conducted

with an apolar liquid of known γ_L and γ_L^{LW}. (In fact, $\gamma_L=\gamma_L^{LW}$, γ_L^+ and γ_L^- are zero.) In this case, Eq. [1.53] can be solved to determine the values of γ_S^+ and γ_S^- by solving two rather than three simultaneous equations.

Once the three surface tensions, i.e., γ_S^{LW}, γ_S^+, and γ_S^-, are known, one can determine the surface tension of the solid, γ_S, as follows:

$$\gamma_S = \gamma_S^{LW} + 2\sqrt{\gamma_S^+\gamma_S^-} \qquad [1.55]$$

Table 1.3 shows the surface tension parameters and components of a number of liquids taken from literature that can be used in the contact angle measurements using various techniques (21). The surface free energy components of various polar and apolar solid surfaces obtained from OCG thermodynamic approach are given in Table 1.4 (21, 26, 94-95, 97).

1.2.2 Contact Angle Measurements

As discussed in the foregoing section, it is essential to be able to measure the contact angle (θ), if one wishes to characterize the surface of a solid in terms of its surface free energy components. There are several different methods of measuring it. The measurement method chosen depends on which form the solid of interest is available. Sessile drop and captive bubble techniques are widely used for the flat surfaces. The Wilhelmy plate technique developed by Neumann is also widely used to determine the advancing and receding contact angles on the flat (or plate) surfaces (98).

1.2.2.1 Sessile Drop and Captive Bubble Techniques

The easiest methods of measuring contact angles on solid surfaces are the sessile drop and the captive bubble techniques, both of which require that the surface of the solid be flat. In the sessile drop technique, a liquid droplet is placed on the surface of a solid of interest and the angle is measured through the liquid phase, as illustrated in Figure 1.1. In this technique, the estimate of the contact angle, θ, is made from the tangential line formed between the solid surface and the sessile drop profile where the drop intersects the surface by means of a comparator microscope fitted with a goniometer scale.

Recently, the sessile drop resting on a horizontal solid surface have been analyzed using the photographic or digital images to get information about the drop shape and dynamic contact angle value (99-102).

Figure 1.1 shows that a finite contact angle is formed when a drop of liquid is brought into contact with a flat solid surface, the final shape of the drop depending on the relative magnitudes of the molecular forces that exist within the liquid (cohesive) and between liquid and solid (adhesive). Thus, the contact angle is a measure of the competing tendencies of the liquid drop and solid determining whether it spreads over the solid surface or rounds up to minimize its own area. For example, when a low surface energy liquid wets a solid surface (i.e, $\gamma_L<\gamma_S$), giving a zero contact angle, the molecular adhesion between solid and liquid is greater than the cohesion between the molecules of the liquid. On the contrary, liquids with high surface tension (i.e, $\gamma_L>\gamma_S$) tend to give a finite (non-zero) contact angle, indicating that the cohesive force is greater than the energy of adhesion between liquid and solid [21]. The figure also illustrates the importance of acid-base interactions on the value of contact angle, hence on the magnitude of adhesion. The concept of the equilibrium of the surface forces is expressed mathematically by Young's equation (Eq. [1.50]).

In the captive bubble technique, the solid is immersed on the surface of a liquid and an air bubble (or drop of another liquid) is brought to the solid/liquid interface. If the surface is hydrophobic, the bubble will stick to the surface. The angle between the surface of the solid and the air bubble is then measured through the liquid phase from either photographs of the bubble profile, or directly, by means of a goniometer telemicroscope (98). The main advantage of this technique is that there is no question that the solid-vapor interface is in equilibrium with the saturated vapor pressure of the liquid.

1.2.2.2 Wilhelmy Plate Technique

A third method, which is developed by Neumann (98), consists of dipping a solid into a liquid and measure the height *(h)* of a liquid rising along the surface. If the surface tension *(γ_L)* and the density *(ρ)* of the liquid are known, one can use the following equation (103) to calculate the contact angle θ:

$$1-\sin\theta=\frac{h^2\rho g}{2\gamma_L}, \qquad [1.56]$$

where *g* is the gravitational acceleration. This method, which is known as *Wilhelmy plate* method, also requires that a flat surface is available. It has been reported that this method is capable of measuring contact angles to 0.1^o precision (98). The Wilhelmy plate technique is suitable for measuring contact angles as a function of temperature (103). With this technique, both advancing and receding contact angles could be measured by moving the plate up or down positions, leaving the position of the line of contact essentially unchanged.

1.2.2.3 Capillary Rise and Thin Layer Wicking Techniques

If a solid in question exists only in powdered form, none of the above can be used to measure its contact angle. In one method, a powdered solid is packed into a capillary tubing, one end of which is subsequently immersed into a liquid of known surface tension. The liquid will rise through the capillaries formed in between the particles within the tubing. The distance *l* traveled by the liquid as a function of time *t* is measured. If one knows the mean radius r^* of the capillaries present in the tubing, he can calculate the contact angle using the Washburn equation (22, 98, 104):

$$l^2=\frac{\gamma_{LV}r^*t\cos\theta}{2\eta}, \qquad [1.57]$$

where η is the liquid viscosity. The derivation of Washburn equation (Eq. [1.57]) is made as follows:

The rate of penetration of a liquid (*v*) into a capillary under laminar flow conditions can be given by (30)

$$v=\frac{dl}{dt}=\frac{r\ \Delta P}{8\eta l} \qquad [1.58]$$

where r is the radius of the circular capillary and ΔP the pressure gradient across the curved interface. The pressure gradient, ΔP, term can be expressed as

$$\Delta P = \frac{2\gamma_L \cos\theta}{r} + \Delta p \qquad [1.59]$$

if the liquid penetrates exclusively under the influence of the surface tension of the liquid and an external pressure difference Δp over the capillary. Eq. [1.59] is known as the *Laplace equation*, i.e, when $\Delta p=0$.

Substituting Eq. [1.59] into Eq. [1.58] and integrating with the boundary conditions $l=0$ and $r=0$ gives

$$l^2 = \frac{r^2}{4\eta}\left\{\frac{2\gamma_L \cos\theta}{r} + \Delta p\right\}t \qquad [1.60]$$

Since a powder bed in a tubing may be considered to consist of a bundle of capillaries with varying radii, an effective radius r^* is substituted for r. For a given particle bed the value of r^* will be constant. The r^*, here, takes into account all the randomly oriented capillaries and other errors introduced by the simplification of the assumption. In such a case, Eq [1.60] is given in the form of

$$l^2 = \frac{r^{*,2}}{4\eta}\left\{\frac{2\gamma_L \cos\theta}{r^*} + \Delta p\right\}t \qquad [1.61]$$

In the capillary rise method l^2 is measured as a function of time t as a given value of Δp. In most cases, experiments are conducted with $\Delta p=0$ and, therefore Eq. [1.61] will take the form of Eq. [1.57] which is known as the Washburn equation for determining the values of contact angles on powdered solid surfaces.

The value of r^* can be obtained by using a liquid which is known completely wet the powder, i.e., $\theta=0$. The completely wetting liquid may be chosen from low energy liquids such as alkanes (hexane, heptane, octane etc.).

The capillary rise technique has frequently been used on mineral powders (22-24, 104). Bruil and van Aartsen [22] studied the surfaces of polyethylene terephthalate (PETP), polyamide (nylon 11), aluminum and graphite powders treated with varying amounts of sodium dodecyl sulfate and measured the contact angles. Crawford et al. [24] determined the contact angles on partially methylated quartz plates and particles with varying surface coverage. The advancing contact angles measured on methylated quartz plates and particles were in good agreement.

One problem with this technique might be the uncertainty associated with determining r^*. There is no guarantee that the value of r^* determined with a completely wetting liquid is indeed zero. Reproducibility and repeatability of test results also depend on the shape and size of the particles. It has been stated that monosized and spherical particles give more reproducible results [25, 104]. However, particle bed disturbances and skewing may be observed when the particles are extremely fine and platy in shape leading to unrealistic values of contact angles. It should be mentioned here that the method of using the Washburn equation gives only advancing contact angles rather than equilibrium or receding contact angles.

Van Oss et al (25) developed an extremely useful alternate technique where only polydispersed suspensions of irregularly shaped particles are available for determining contact angles. It is named as the "thin layer wicking" technique. Similar to the capillary rise technique, the thin layer wicking technique uses the Washburn equation for obtaining the values of contact angles on powdered solid surfaces. In this technique, a powdered sample is deposited on a microscopic glass slide in the form of aqueous slurry. After drying the sample, one end of the glass slide is immersed vertically in a liquid. The liquid starts to creep up the slide through the capillaries formed between the particles deposited on the glass surface. The velocity at which a liquid creeps up the slide is measured, and then converted to a contact angle using the Washburn equation (Eq. [1.57]).

The value of r^* in the Washburn equation can be obtained by using completely spreading liquids (apolar) such as hexane, heptane, octane, decane and dodecane. In this case, it is considered that cosθ=1. For each powdered solid surface, the $2\eta l^2/t$ vs. γ_L for alkanes should yield a straight line whose slope is the mean pore radius (r^*) (25-26). Once the value of r^* is known, it is then possible to calculate the value of the contact angle for a given liquid on the powdered talc surface using the Washburn equation (Eq. [1.57]). The contact angle liquids can be chosen from high-energy polar (e.g., water, formamide, ethylene glycol) and nonpolar liquids (e.g. methylene iodide and 1-bromonaphthalene) for the wicking measurements.

1.2.2.4 Contact Angle Determination From Heat of Immersion

Another technique of measuring contact angles for powders is to measure the heat generated when a powder is immersed in a liquid. A microcalorimeter may be used to measure the heat effect (h_i) created by wetting powdered talc samples with various liquids such as water and n-heptane. By dividing h_i with the total surface area of the sample used in the experiment, one obtains the heat of immersional wetting ($-\Delta H_i$) given in units of mJ/m^2.

Consider a solid is suspended over a liquid in a closed container. In this case, the solid surface will be in equilibrium with the liquid vapor. Imagine now that the solid is immersed into the liquid. The free energy change (ΔG_i) associated with this process may be given by the following relationship:

$$\Delta G_i = \gamma_{SL} - \gamma_{SV}\,, \qquad [1.62]$$

in which γ_{SL} is the solid/liquid interfacial tension and γ_{SV} is the solid/vapor interfacial tension.

When a solid is immersed into a liquid from its own vapor phase (i.e., the solid is not exposed to the vapor phase of the liquid by which it is wetted, or the solid is in vacuum), the free energy ΔG_i of immersional wetting is given by the following relationship:

$$\Delta G_i = \gamma_{SL} - \gamma_S \qquad [1.63]$$

where γ_S is the surface free energy of the solid, which is in equilibrium with its own vapor.

Of the two different free energies represented by Eqs. [1.62] and [1.63], the latter is more useful in that it can be related to the heat ($-\Delta H_i$) of immersion that can be readily measured in experiment. The heat of immersion is routinely measured by immersing a powdered solid in vacuum into a liquid.

The enthalpy of immersion (ΔH_i) determined using the heat of immersion measurement can be related to ΔG_i as follows:

$$\Delta H_i = \Delta G_i - T\left(\frac{d\Delta G_i}{dT}\right)_p \qquad [1.64]$$

where T is the absolute temperature. Substituting Eq. [1.63] into Eq. [1.64], one obtains:

$$\Delta H_i = (\gamma_{SL} - \gamma_S) - T\left[\frac{d(\gamma_{SL} - \gamma_S)}{dT}\right]_p \qquad [1.65]$$

Substituting Eq. [1.50] into [1.65],

$$\begin{aligned}\Delta H_i &= -\gamma_L \cos\theta + T\left[\frac{\partial(\gamma_L \cos\theta)}{\partial T}\right]_p \\ &= -\gamma_L \cos\theta + T\left[\cos\theta\left(\frac{\partial\gamma_L}{\partial T}\right)_p + \gamma_{LV}\left(\frac{\partial\cos\theta}{\partial T}\right)_p\right] \\ &= -\cos\theta\left[\gamma_L - T\left(\frac{\partial\gamma_L}{\partial T}\right)_p\right] + \gamma_L T\left(\frac{\partial\cos\theta}{\partial T}\right)_p\end{aligned} \qquad [1.66]$$

Since the enthalpy of the liquid (H_L) is given by

$$H_L = \gamma_L - T\left(\frac{\partial \gamma_L}{\partial T}\right)_p, \qquad [1.67]$$

Eq. [1.66] is reduced to:

$$\Delta H_i = -H_L \cos\theta + \gamma_L T\left(\frac{\partial \cos\theta}{\partial T}\right)_p \qquad [1.68]$$

Solving Eq. [1.68] for $\cos\theta$, one obtains the following relationship:

$$\cos\theta = \frac{1}{H_L}\left[\gamma_L T\left(\frac{\partial \cos\theta}{\partial T}\right)_p - \Delta H_i\right], \qquad [1.69]$$

which is a first-order differential equation with respect to cosθ. Eq. [1.69] have been derived by Adamson (98) and used by Malandrini et al (29) for determining contact angles on various talc samples from Europe by ignoring the $\partial \cos\theta / \partial T$ term. However, the methodology used by Malandrini et al (29) is erroneous because of the assumptions made in converting the heat of immersion to free energy of immersion.

There are no analytical solutions for Eq. [1.69]. Numerical solutions are possible, provided that a value of contact angle is known at one particular temperature. Nevertheless, Eq. [1.69] can be useful for determining θ from the value of ΔH_i determined using a calorimeter. For this to be possible, it is necessary to have the values of H_L, γ_{LV} and $\partial cos\theta/\partial T$ for a given liquid at a given temperature. The first two are usually available in the literature.

There are several ways of determining temperature coefficient of $cos\theta$. *First*, one measures θ on polished solid surfaces as a function of temperature and determine $\partial cos\theta/\partial T$ experimentally. An assumption made here is that although contact angle may change when the solid is pulverized, its temperature coefficient may remain the same. *Second*, the contact angle of a powdered sample is measured by pressing it into a pellet. Again, the pressed solid sample may have a different contact angle from that of lose powders. However, its temperature coefficient may be assumed to remains the same.

Third, the contact angles of powdered samples are measured using the capillary rise technique. This technique gives advancing rather than equilibrium contact angles. If one uses this technique to determine $\partial cos\theta/\partial T$, an implicit assumption is that the temperature coefficients of the equilibrium and the advancing angles are the same.

Adamson (2, 98) related the heat of immersion enthalpy which can be readily measured by a microcalorimeter (Eq. [1.65]) to the contact angle, θ, through the application of Young's equation (Eq. [1.50]) as follows:

$$H_i = -\gamma_L \cos\theta - (\gamma_S - \gamma_{SV}) - T\left(\frac{\partial \gamma_{SL}}{\partial T} - \frac{\partial \gamma_S}{\partial T}\right) \qquad [1.70]$$

Since in practice, γ_S-γ_{SV} and $\partial\gamma_S/\partial T$ are negligibly small for systems having large contact angles and also the value of $\partial\gamma_{SL}/\partial T$ assumed to be relatively constant for low energy surfaces, i.e, $\partial\gamma_{SL}/\partial T=0.07\pm0.02$ mJ m^{-2} K^{-1}, a simple relationship between contact angle and heat of immersion enthalpy can be established as:

$$\cos\theta = \frac{-0.07T - H_i}{\gamma_L} \qquad [1.71]$$

Eq [1.71] has been shown to work well for low energy (nonpolar) solids such as graphon (27), teflon (105), fluorinated hydrocarbons (30) and methylated silica surfaces (31).

1.2.3 Limitations of Contact Angle Measurements

1.2.3.1 Spreading Pressure

One of the major problems in the use of Young's equation is that its assumption of $\gamma_S \approx \gamma_{SV}$. This may or may not be the case, depending on the experimental conditions. In particular, the surface free energy of solid can significantly be reduced as a result of the adsorption of the vapors of the wetting liquid (at saturation) onto the solid surface. When the solid surface is in equilibrium with the liquid vapor, the reduction of the

surface free energy of the solid due to the vapor adsorption is termed the equilibrium spreading pressure, π_e, and hence its addition into Eq. [1.50] leads to the modified Young equation:

$$\gamma_L cos\theta = \gamma_S - \gamma_{SL} + \pi_e \qquad [1.72]$$

where $\pi_e = \gamma_S - \gamma_{SV}$. Thus, the reduction in the value of the ideal surface free energy of a solid (γ_S) due to the adsorption of liquid vapor onto the solid surface can be measured as a function of π_e [21, 83]. The distinction between γ_S and γ_{SV} seems first to have been made by Bangham and Razouk (106). Later, the difference between the two (or the value of π_e) has been determined on various high- and low-energy solids by other investigators (25-26, 107- 110).

The equilibrium spreading pressure may be measured experimentally from the adsorption isotherms for the vapors of the liquid on the solid surface, $\Gamma = \Gamma(p)$, where p is the partial pressure of the vapors of the liquid, using the Gibbs adsorption equation [98]:

$$\pi_e = \gamma_S - \gamma_{SV} = RT \int_0^P \Gamma d \ln P \qquad [1.73]$$

where P is the saturation vapor pressure of the liquid. However, the measurement of π_e is cumbersome and is not, in general, a simple task on a macroscopic solid surface and its theoretical estimation is difficult.

It is, therefore, common among the investigators to assume that π_e should be negligible for all cases in which the contact angle is finite, i.e., for so-called smooth, homogenous, hydrophobic low energy surfaces [25, 108]. Fowkes et al [108] studied the possibility of spreading pressures arising with high-energy liquids (e.g. water vapor) deposited on low-energy solids, and found that this did not occur. On the other hand, when the vapor of a low-energy liquid (e.g. cyclohexane or heptane) could interact with a somehow higher-energy solid surface, the effect of resulting positive spreading pressure caused an increase in the contact angle of water on that solid surface, which allowed the

determination of π_e [108]. Van Oss et al. [25] also showed by conducting thin layer wicking measurements, with non-spreading liquids (i.e. $\gamma_L > \gamma_S$ and $\cos\theta < 1$) neither spreading nor pre-wetting takes place on low-energy solid surfaces. Thus, it appears not to be justified to take the equilibrium spreading pressures into account, under non-spreading conditions.

It has been shown, however, that substantially positive π_e values could exist with non-spreading liquids [111, 112]. Busscher et al [111] studied the adsorption of water and propanol on various solid surfaces using ellipsometry technique. The authors showed that even when $\gamma_L > \gamma_S$, spreading pressures can have a considerable effect on the contact angle value. They correlated the adsorption of water and propanol on solid surfaces with equilibrium spreading pressures. They found that the equilibrium spreading pressures are in the same order of magnitude for water and for propanol on both high- and low-energy surfaces. However, it is well known that the spreading behavior of low-energy liquids (e.g, propanol, $\gamma_{propanol} = 23.7$ mJ/m^2) differs fundamentally from the high-energy liquids (e.g., water, $\gamma_{water} = 72.8$ mJ/m^2), especially on solids with $\gamma_S \approx 35 \pm 10$ mJ/m^2 (Fowkes et al., [108]). Fowkes et al (108) showed that the vapor of water does not spread over low energy polymers, whereas cyclohexane vapor spreads over the polymer surface. Thus, the correlation between the ellipsometric results and the equilibrium spreading pressures, particularly when using alcohol-water mixtures, must be regarded as questionable. It appears that π_e can be neglected in cases where $\gamma_L > \gamma_S$, and where vapors of low-energy substances are absent.

1.2.3.2 Surface Heterogeneity – Contact Angle Hysteresis

It has been shown that the wetting process can be assumed as an adsorption-desorption process (2, 21, 113). A drop of liquid, which is placed on a solid surface, spreads until equilibrium is attained. If additional liquid is added to the drop, the contact line advances and eventually stops. Each time the motion of drop ceases (i.e. within a few seconds), the drop exhibits an advancing contact angle θ_a. Alternatively, if liquid is withdrawn from the drop using a syringe the contact angle decreases without movement of the contact line. If a large amount of liquid withdrawn, the contact angle would start retreating. When the motion ceases, the drop exhibits a receding contact angle θ_r. This is

illustrated schematically in Figure 1.2. Obviously, the drop size has an effect on the measured contact angle value.

The difference between θ_a and θ_r is called the contact angle hysteresis and is defined empirically as an arithmetic difference between the two (102, 113),

$$\Delta\theta = \theta_a - \theta_r \qquad [1.74]$$

The contact angle hysteresis is usually attributed to chemical and morphological heterogeneity of surface, roughness, swelling, rearrangement, inter-diffusion and/or surface deformation (21, 98, 114-118). For ideally smooth and homogenous solid surfaces, the values of θ_a and θ_r should be very close. However, the difference between θ_a and θ_r can be quite large, as much as 50^o for water on mineral surfaces, suggesting surface heterogeneity (2). The contact angle hysteresis can be quite important in various industrial applications, e.g., coating etc.

It has been suggested that both advancing and retreating contact angles should be measured wherever possible. Because, there is likely to be chemical information residing in retreating contact angle data that is different from the information in advancing contact angles for the same solid surface. In general, if the solid surface is smooth, θ_a is used as a measure of apolar aspect of surface (low surface energy sites), while θ_r of its polar aspects (high surface energy sites), as θ_a is always larger than θ_r (2, 29, 83, 93). However, it is generally assumed that the Young's equation is valid for contact angles measured as the advancing angles (11, 21, 83, 102, 119). In some publications equilibrium contact angles (θ_e) are measured (120-121), but they are not necessarily equal to the contact angle which is used in Young's equation (102).

For solid surfaces with heterogeneities due to impurities or polycrystallinity, Cassie equation can be used to model the surface over small length scales (2, 24),

$$\cos\theta_A = f_1 \cos\theta_1 + f_2 \cos\theta_2 \qquad [1.75]$$

where θ_A is the average contact angle measured on the heterogeneous surface, and $f_1+f_2=1$, while θ_1 and θ_2 are the contact angles one would measure on a solid surface solely consisting of material, 1, and of material, 2, respectively. In general,

$$\cos\theta_A = \sum_{i=1}^{n} f_i \cos\theta_i \qquad [1.76]$$

for an *n* region surface (24, 122). Another averaging expression has been proposed (21)

$$[1+\cos\theta_A] = f_1(1+\cos\theta_1)\gamma_L + f_2(1+\cos\theta_2)\gamma_L \qquad [1.77]$$

which is equivalent to Cassie's equation (Eq. [1.75]).

Recently, some investigators have proposed modifications of Cassie's equation (123-124). However, it has been reported that Cassie's equation, in the form of Eq. [1.75], correlates well with a variety of experimental situations (2, 21, 125-129) and it seems reasonable to use it without modification.

1.2.4 Contact Angle, Surface Hydrophobicity and Surface Free Energies

Direct surface force measurements conducted on various solid surfaces have shown that the macroscopic hydrophobicity of a surface (as measured by contact angle θ value) and the magnitude of the hydrophobic force are uniquely related (130-134). It has also been shown that as the water contact angle value increases, the value of γ_S decreases (17-19, 21, 26, 95-96). However, the relationship between the contact angle and, the surface hydrophobicity and surface free energy components, γ_S^{LW}, γ_S^{AB}, γ_S^-, γ_S^+ was not fully established with the exception of one study. The work has been done, recently, at Virginia Tech by Pazhianur (135) should be addressed in this regard. Pazhianur conducted direct force measurements between methylated silica plates with varying hydrophobicities and a hydrophobic glass sphere ($\theta_a=109^o$) that has been used to simulate the air bubble, and contact angle measurements on methylated silica surfaces with varying hydrophobicities. Figure 1.3 shows a plot taken from the work of Pazhianur where the K (hydrophobicity constant) values obtained from force measurements and

surface free energy components of methylated silica surfaces obtained from Van Oss-Chaudhury-Good (OCG) thermodynamic approach, plotted as a function of the advancing water contact angle (θ_a). According to Figure 1.3: i) the value of K increases as θ_a increases, ii) the increase in the value of θ_a is essentially due to a decrease in the values of both Lifshitz-van der Waals (γ_S^{LW}) and Lewis acid-base (γ_S^{AB}) surface free energy components. Essentially, Pazhianur argued that the magnitude of hydrophobicity constant (K) and the γ_S^{LW} and γ_S^{AB} surface free energy components were strictly dependent on the θ_a exhibited by a solid surface.

1.3 REPORT ORGANIZATION

The results obtained in the present work have been reported in Chapters 2 to 5. Each chapter comprises of an introduction, experimental, results and discussion, and conclusion sections, and may be considered as an article for publication. In Chapter 2 the results of direct contact angle measurements conducted on various flat and powdered talc surfaces and surface free energy components obtained using Van Oss-Chaudhury-Good (OCG) thermodynamic approach on these surfaces are reported. It was found that the surface hydrophobicity of talc increases with decreasing particle size. On the other hand, both the Lifshitz-van der Waals (γ_S^{LW}) and the Lewis acid-base (γ_S^{AB}) surface free energy components and, hence, total surface free energy (γ_S) on talc surface decrease as the particle size decrease associated with increase in the values of contact angles. The increase in the surface hydrophobicity of talc and decrease in the values of total surface free energy (γ_S) and its components (γ_S^{LW} and γ_S^{AB}) is attributed to the exposure of more basal plane surfaces upon pulverization. It was also found that the Lewis electron-donor (γ_S^-) component on talc surface is much higher than the Lewis electron-acceptor (γ_S^+) component, suggesting surface basicity of talc.

In Chapter 3 heat of immersion measurements were conducted by a flow microcalorimeter on a number of powdered talc surfaces using various liquids. The heats of immersion values were then converted to the contact angles using a rigorous thermodynamic relation. The measured heat of immersion values in water and contact angles showed that the surface hydrophobicity of talc samples increase with decreasing particle size, which confirms the findings of Chapter 2. A relationship between

advancing water contact angle θ_a, and surface free energies and heat of immersion ($-\Delta H_i$) was established. It was found that i) the value of $-\Delta H_i$ decrease as θ_a increases, ii) the increase in the value of θ_a is essentially due to a decrease in the values of both Lifshitz-van der Waals (γ_S^{LW}) and Lewis acid-base (γ_S^{AB}) surface free energy components. The most interesting finding was that the basic surface component (γ_S^-) on talc surface increased with increasing θ_a, while the acid component (γ_S^+) slightly decreased.

In Chapter 4 the heats of adsorption of butanol on various talc samples from n-heptane were determined using a flow microcalorimeter. The heats of adsorption values were used to estimate % hydrophilicity and hydrophobicity and the areal ratio (the ratio between basal and edge surface area) values of various talc samples. In addition, contact angle measurements and heat of butanol adsorption measurements were conducted on a run-of-mine talc sample that is ground to two different particle size fractions, i.e, d_{50}=12.5 μm and d_{50}=3.0 μm, respectively. The results were used to estimate the surface free energy components at the *basal* and *edge* surfaces of talc. It was found that the total surface free energy (γ_S) at the basal plane surface of talc is much lower than the total surface free energy at the edge surface. The results of the work suggest also that the basal surface of talc is *monopolar basic*, while the edge surface is *monopolar acidic*. The results explain why the basicity of talc surface increases with decreasing particle size as defined in Chapter 3, simply due to the increased basal plane surfaces that are basic in character. It has to be noted that this information becomes available for the first time in the present work.

Chapter 5 is a summary of test work done on the east Georgia kaolin clay in order to investigate the possibility of removing discoloring impurities such as anatase (TiO_2) and iron oxides and producing high-brightness clay with GE brightness higher than 90% using flotation and selective flocculation techniques. The results of the work show that a clay product with +90% brightness can readily be obtained with recoveries (or yields) higher than 80% using selective flocculation technique. It was found that the proper control of surface hydrophobicity of anatase, which is a main discoloring impurity found in east Georgia kaolin, is crucially important for a successful flotation and selective flocculation process. Heat of immersion and contact angle measurements conducted on anatase surface showed: i) the magnitude of the contact angle value, and hence surface

free energy and its components on anatase surface is critically dependent on the amount of surfactant (e.g. hydroxamate) used for the surface treatment, ii) as the concentration of hydroxamate increases from 2 lb/t to 4 lb/t the surface becomes more hydrophobic and the γ_S decreases. Due to a decrease in the value of γ_S with increasing surface hydrophobicity, the Gibbs free energy of interaction ($-\Delta G_{131}$) between two anatase particles in water increases, and so does the efficiency of the separation process.

Finally, Summary and Conclusions and Future Work are given in Chapters 6 and 7, respectively.

1.4 REFERENCES

1. Good, R. J., and van Oss, C. J., in *Modern Approaches to Wettability: Theory and Applications*, Eds: M. E. Schrader, and G. Loeb, Plenum Press, New York, pp. 1-27, 1992.
2. Adamson, A. W. and Gast, A.P., *Physical Chemistry of Surfaces*, 6th ed., John Wiley and Sons, 1997.
3. Janczuk, B, Wojcik, W., Zdziennicka, A., *J. of Colloid and Interface Science*, 157, 384-393, 1993.
4. Padday, J. F., (Ed), *Wetting, Spreading, and Adhesion*, Academic Press, New York, 1978.
5. Zisman, W. A., in: *Handbook of Adhesives*, Skeist, I., Ed: van Nostrand, NewYork, Chapter 3, 1977.
6. Fowkes, F.M., *Industrial and Engineering Chemistry*, 56/12, 40, 1964.
7. Fowkes, F.M., *J. of Adhesion*, 4, 153, 1972.
8. Van Oss, C. J., Chaudhury, M. K., and Good, R. J., *J. Separation Sci. and Technology*, 22, 1, 1987.
9. Van Oss, C. J., Good, R. J., and Chaudhury, M. K., *Langmuir*, 4, pp. 884-891, 1988.
10. Van Oss, C. J., Chaudhury, M. K., and Good, R. J., *J. Colloid Interface Science*, 128, 313, 1989.

11. Neumann, A. W. and Good, R.J., *Techniques of Measuring Contact Angles, Surface and Colloid Science*, Volume II, *Experimental Methods*, Eds: R.J. Good and R. R. Stromberg, Plenum Pres, New York, 1979.
12. Fuerstenau, D. W., *Mining Engineering*, Transactions AIME, December, pp. 1367-1367, 1957.
13. Leja, J., *Surface Chemistry of Froth Flotation*, Plenum Press, New York, 1982.
14. Yoon, R.-H., *Aufbereitungs-Technik*, 32, 474, 1991.
15. Yoon, R.-H., and Ravishankar, S. A., *J. Colloid Interface Science*, 179, 391, 1996.
16. Yoon, R.-H., and Pazhianur, R., *Colloid Surfaces*, 1999.
17. Van Oss, C. J., Giese, R. F., and Good, R. J., *Langmuir*, 6, pp. 1711-1713, 1990.
18. Spelt, J. K., Li, D., and Neumann, A. W., in *Modern Approaches to Wettability: Theory and Applications*, Eds: M. E. Schrader, and G. Loeb, Plenum Press, New York, pp. 101-142, 1992.
19. Bilinski, B., and Chibowski, E., *Powder Technol.*, 31, 39, 1983.
20. Yoon, R.- H. and Yordan, J. L., *J. of Colloid and Interface Science*, Vol. 146, No. 2, pp. 101-108, 1991.
21. Van Oss, C. J., *Interfacial Forces in Aqueous Media*, Marcel Decker Inc., New York, 1994.
22. Bruil, H. G., and van Aartsen, J. J., *Colloid & Polymer Science*, 252, pp. 32-38, 1974.
23. Hansford, D. T., Grant, D. J. W., and Newton, J. M., *J. C. S. Faraday I*, 76, 2417-2431, 1980.
24. Crawford, R., Koopal, L. K. and Ralston, J., *Colloids and Surfaces*, 27, 57-64, 1987.
25. Van Oss C.J., Griese, R.F. Jr., Li, Z., Murphy, K., Norris, J., Chaudhury, M. K., and and Good, R. J., *J. Adhesion Sci. and Technology*, Vol. 6, No.4, 413-428, 1992.
26. Wu, W., Griese, R.F. Jr., and van Oss C.J., *Powder Technology*, 89, 129-132, 1996.
27. Young, G. J., Chessick, J. J., Healey, F. H., and Zettlemoyer, A. C., *J. Phys. Chem.*, 58, 313, 1954.
28. Fowkes, F.M., *Ind. and Eng. Chem.*, 56/12, 40, 1967.

29. Malandrini, H., Clauss, F., Partyka, S., and Douillard, J. M., *J. Colloid and Interface Sci.*, 194, 183-193, 1997.
30. Spagnolo, D. A., Maham, Y., Chuang, K. T., *J of Physical Chemistry*, 100, 6626, 1995.
31. Yan, N., Maham, Y., Masliyah, J. H., Gray, M., and Mather , A. E., *J of Colloid and Interface Sci.*, 228, pp.1-6, 2000.
32. Groszek, A. J., *Carbon*, Vol. 25, No.6, pp. 717-722, 1987.
33. Groszek, A. J., and Templer, C. E., *Fuel*, Vol. 67, pp. 1658-1662, 1988
34. Groszek, A. J., and Partyka, S., *Langmuir*, 9, pp. 2721-2725, 1993.
35. Basilio, C., *Ph.D. Thesis*, Virginia Tech, 1989.
36. Fowkes, F. M., and Joslin, S. T., *see Ref. 75*, 1983.
37. Malhammar, G., *Colloids and Surfaces*, 44, pp. 61-69, 1990.
38. Zettlemoyer, A. C., in *Surfaces and Coatings Related to Paper and Wood*, Eds: R. H. Marchessault and C. Skaar, Syracuse University Press, 1967.
39. Botero, J. Y., Bruant, M., and Cases, J. M., *J of Colloid and Interface Sci.*, 124, 515, 1988.
40. Celik, M. S. and Yoon, R.-H., *Langmuir*, Vol. 7, No. 8, pp. 1770-1774, 1990.
41. Sanders, N. D., *J. of Pulp and Paper Sci.*, Vol. 18, No. 5, pp. 168-175, 1992.
42. Moudgil, B. M., Behl, S., and Kulkarni, S., *J of Colloid and Interface Sci.*, 148, pp. 337-341, 1992.
43. Van der Waals, J. D., 1873, in Ref. 21.
44. Van der Waals, 1899, in Ref. 21.
45. Keesom, W. H., *Phys. Z.*, 22, 643, 1921.
46. Debye, P., *Phys. Z.*, 21, 178, 1920.
47. London, F., *Z. Phys. Chem.*, 11, 222, 1930.
48. London, F., *Trans. Faraday Soc.*, 33, 8, 1937.
49. Overbeek, J. Th. G., in *Colloid Science*, Ed: H. R. Kruyt, Elsevier, Amsterdam, 1, 245, 1952
50. Fowkes, F.M., in: *Physicochemical Aspects of Polymer Surfaces*, Ed: K.L. Mittal, vol. 2, p. 583, Plenum Press, New York, 1983.

51. Israelachvili, J. N., *Intermolecular and Surface Forces*, Second Edition, Academic Press, London, 1991.
52. Hamaker, H. C., *Physica*, 4, 1058, 1937.
53. Berthelot, D., *Comp. Rend. Acad. Sci.*, 126, 1703, 1898.
54. Nir, S., *Progr. Surface Sci.*, 8, 1, 1976.
55. Visser, J. *Adv. Colloid Interface Sci.*, 3, 331, 1972.
56. Neumann, A. W., Omenyi, S. N., and Van Oss, C. J., *Colloid Polymer Sci.*, 257, 413, 1979.
57. Van Oss, C. J., Omenyi, S. N., and Neumann, A. W., *Colloid Polymer Sci.*, 257, 737, 1979.
58. Israelachvili, J. N., *Intermolecular and Surface Forces: With Applications to Colloidal and Biological Systems*, Academic Press, London, 1985
59. Fowkes, F. M., and Pugh, R. J., in *Polymer Adsorption and Dispersion Stability*, Eds: E. D. Goddard and B. Vincent, American Chemical Society, 1984.
60. Hough, D. B., and White, L. R., *Adv. Colloid Interface Sci.*, 14, 3, 1980.
61. Van Oss, C. J., and Good, R. J., *Colloids and Surfaces*, 8, 373, 1984.
62. Van Oss, C. J., Chaudhury, M. K., and Good, R. J., *Chem. Revs.*, 88, 927, 1988.
63. Padday, J. F., and Uffindell, N. D., *J. Phys. Chem.*, 72, 1407, 1968.
64. Lifshitz, E. M., *J. Exp. Theor. Phys.*, 29, 94, 1955.
65. Rytov, S. M., *Theory of Electric Fluctuations and Thermal Radiations*, Moscow Academy of Science Press, Moscow, 1953.
66. Israelachvili, J. N., *Q. Rev. Biophys.*, 6, 341-387, 1974.
67. Grifalco, L. A., and Good, R. J., *J. Phys. Chem.*, 61, 904, 1957.
68. Fowkes, F. M., *J. Phys. Chem.*, 67, pp. 2538-2541, 1963.
69. Fowkes, F. M., Ronay, G. S., and Schick, M. J., *J. Phys. Chem.*, 63, 1684, 1959.
70. Fowkes, F. M., *J. Phys. Chem.*, 64, 726, 1960.
71. Bolger, J. C., and Michaels, A. S., *Interface Conversion for Polymer Coatings*, Ed: P. Weiss, pp. 3-60, Elsevier, New York, 1968
72. Lipatov, Y. S., and Sergeeva, L. M., *Adsorption of Polymers*, Halsted, New York, 1974.
73. Sorensen, P., *J. Paint Technol.*, 47, 31, 1975.

74. Fowkes, F. M., and Mostafa, M. A., *Ind. Eng. Chem. Prod. Res. Dev.*, 71, pp. 3-7, 1978.
75. Fowkes, F. M., *J. Adhes. Sci.*, 1, pp. 7-27, 1987.
76. Van Oss, C. J., Good, R. J., and Chaudhury, M. K., *J. of Colloid and Interface Science*, 111, pp. 378, 1986.
77. Van Oss, C. J., Chaudhury, M. K., and Good, R. J., *Adv. Coll. Interface Sci.*, 28, pp. 35-64, 1987.
78. Van Oss, C. J., Chaudhury, M. K., and Good, R. J., J. *of Colloid and Interface Science*, 128, 313, 1988.
79. Fowkes, F. M., *J. Phys. Chem.*, 66, 382, 1962.
80. Johnson, R. E., Jr., and Dettre, R. H., *Langmuir*, 5, 293, 1989.
81. Janzcuk, B., Kerkeb, M. L., Bialopiotrowicz, T., and Gonzalez-Caballero, F., *J. Colloids Interface Sci.*, 151, pp. 333-342, 1991.
82. Janczuk, B., Wojcik, W., and Zdziennicka, A., *J. Colloids Interface Sci.*, 157, pp. 384-393, 1992.
83. Berg, J. C., *Nordic Pulp and Paper Research Journal*, 1, 75-85, 1993.
84. Holländer, A. J., *J. Colloids Interface Sci.*, 169, 493, 1995
85. Morra, M. J., *J. Colloids Interface Sci.*, 182, 312, 1996.
86. Kwok, D. Y., Lee, Y. and Neumann, A. W., *Langmuir*, 14, pp. 2548-2553, 1998.
87. Van Oss, C. J., Chaudhury, M. K., and Good, R. J., *Adv. Colloid Interface Sci.*, 28, 35, 1987.
88. Van Oss, C. J. and Good, R. J., *J. Dispersion Sci. Tech.*, 1988.
89. Fowkes, F. M., in *Surfaces and Interfaces*, Eds: J. J. Burke, Syracuse University Press, 1967.
90. Laskowski, J. S., and Kitchener, J. A., *J. of Colloid and Interface Science*, 29, 670, 1969.
91. Young, T., 1805. *in Ref. 21*.
92. Dupré, A., 1869. *in Ref. 21.*
93. Good, R. J., Srivasta, N. R., Islam, M., Huang, H. T. L., and Van Oss, C. J., *J. Adhesion Sci. Technol.*, Vol. 4, No. 8, pp. 607-617, 1990.
94. Holysz, L., and Chibowski, E., *Langmuir*, 8, pp. 303-308, 1992.

95. Holysz, L., and Chibowski, E., *Langmuir*, 8, pp. 717-721, 1992.
96. Li, Z., Giese, R. F., Van Oss, C. J., Yvon, J., and Cases, J., *J. Colloids and Interface Sci.*, 156, pp. 279-284, 1993.
97. Holysz, L., and Chibowski, E., *J. Colloids and Interface Sci.*, 164, pp. 245-251, 1994.
98. Adamson, A. W., *Physical Chemistry of Surfaces*, 5th ed., John Wiley and Sons, 1990.
99. Amirfazli, A., Chatain, D., and Neumann, A. W., *Colloids and Surfaces*, 142, pp. 183-188, 1998.
100. Del Rio, O. I., Kwok, D. Y., Wu, R., Alvarez, J. M., and Neumann, A. W., *Colloids and Surfaces*, 143, pp. 197-210, 1998.
101. De Ruijter, M., Kölcsh, O., Voué, M., De Coninck, J., and Rabe, J. P., *Colloids and Surfaces*, 144, pp. 235-243, 1998.
102. Kwok, D. Y., Leung, A., Lam., C. N. C., Li, A., Wu, R., and Neumann, A. W., *J. Colloids and Interface Sci.*, 206, pp. 44-51, 1998.
103. Neumann, A. W., and Tanner, W., *J. Colloids and Interface Sci.*, 34, pp. 1-8, 1970.
104. Ku, C. A., Henry, J. D., Siriwardane, R., and Roberts, L., *J. Colloids and Interface Sci.*, 106, pp. 377-385, 1985.
105. Chessick, J. J., Healy, F. H., and Zettlemoyer, A. C., *J. Phys. Chem.*, 60, 1345, 1956.
106. Bangham, D. H., and Razouk, R. I., *Trans. Fraday Soc.*, 33, 1459, 1937.
107. Harkins, W. D., and Livingston, H. K., *J. Chem. Phys.*, 10, 342, 1942.
108. Fowkes, F. M., McCarthy, D. C., and Mostafa, M. A., *J. of Colloid and Interface Science*, 78, 200, 1980.
109. Chibowski, E. and Holysz, L., *J. of Colloid and Interface Science*, 112, pp. 15-23, 1986.
110. Chibowski, E. and Holysz, L., *J. of Colloid and Interface Science*, 127, pp. 377-387, 1989.
111. Busscher, H. J., Kim, K. G. A., Van Silfout, G. A. M., and Arends, J., *J. of Colloid and Interface Science*, 114, 307, 1986.

112. Bellon-Fontaine, M.-N. and Cerf, O., *J. Adhesion Sci. and Technology*, 4, 475, 1990.
113. Extrand, C. W., *J. Colloid and Interface Sci.*, 207, pp. 11-19, 1998.
114. Johnson, R. E. Jr., and Dettre, R. H., *J Phys. Chem.*, 68, 1744, 1964.
115. Dettre, R. H., and Johnson, R. E. Jr., *J Phys. Chem.*, 69, 1507, 1965.
116. Andrade, J. D., Smith, L. M., and Gregonis, D. E., in *Surface and Interfacial Aspects of Biomedical Polymers*, Ed: J. D. Andrade, Vol. 1, Plenum Press, New York, 1985.
117. De Gennes, P. G., *Rev. Mod. Phys.*, 57, 828, 1985.
118. Garbassi, F., Morra, M., and Occhiello, E., *Polymer Surfaces, From Physics to Technology*, Wiley, New York, 1994.
119. Good, R. J., *Surface Colloid Sci.*, 11, 1, 1979.
120. Neumann, A. W., *Adv. Colloids Interface Sci.*, 4, 105, 1974.
121. Marmur, A., *Colloids Surf.*, 116, 25, 1996.
122. Swain, P. S., and Lipowsky, R., *Langmuir,* 14, pp. 6772-6780, 1998.
123. Israelachvili, J. N., and McGee, M. L., *Langmuir*, 5, 288, 1989.
124. Drelich, J., and Miller, J. D., *Langmuir*, 9, 619, 1993.
125. Cassie, A. B. D., and Baxter, S., *Trans. Faraday Soc.*, 40, 456, 1944.
126. Wenzel, R. N., *J. Phys. Chem.*, 53, 1466, 1949.
127. Oliver, J. F., Huh, C. and Mason, S. G., *J. Adhes.*, 8, 273, 1977.
128. Lamb, R. M., and Furlong, D. N., *J. Chem. Soc. Faraday Trans. I*, 8, 61, 1977.
129. Blake, P., and Ralston, J., *Colloids Surfaces*, 15, 11, 1985.
130. Fielden, M. L., Hayes, R. A., and Ralston, J., *Langmuir*, 12, 3721, 1996.
131. Israelachvili, J. N., and Pashley, R. M., *Nature*, 300, 341, 1982.
132. Rabinovich, Ya. I., and Yoon, R.- H., *Langmuir*, 93, 263, 1994.
133. Yoon, R.- H.and Ravishankar, S. A., *J. Colloid and Interface Sci.*, 166, 215, 1994.
134. Yoon, R.- H.and Ravishankar, S. A., *J. Colloid and Interface Sci.*, 179, 401, 1996.
135. Pazhianur, R., *Ph.D. Thesis*, Virginia Tech, 1999.

Table 1.1 Hamaker constants for two identical media interacting across vacuum (51)

Medium	Dielectric Constant	Refractive Index n	Absorption Frequency ν_e (10^{15} s^{-1})	Hamaker constant, A (10^{-20} J)		
				Eq. [1.21] ε_3=1	Exact Solution	Experi-mental
Water	80	1.333	3.0	3.7	3.7, 4.0	
n-Pentane	1.84	1.349	3.0	3.8	3.75	
n-Octane	1.95	1.387	3.0	4.5	4.5	
n-Dodecane	2.01	1.411	3.0	5.0	5.0	
n-Tetradecane	2.03	1.418	2.9	5.0	5.1, 5.4	
n-Hexadecane	2.05	1.423	2.9	5.1	5.2	
Hydrocarbon (crystal)	2.25	1.50	3.0	7.1		10
Cyclohexane	2.03	1.426	2.9	5.2		
Benzene	2.28	1.501	2.1	5.0		
CCl_4	2.24	1.460	2.7	5.5		
Acetone	21	1.359	2.9	4.1		
Ethanol	26	1.361	3.0	4.2		
Polystyrene	2.55	1.557	2.3	6.5	6.6, 7.9	
PVC	3.2	1.527	2.9	7.5	7.8	
PTFE	2.1	1.359	2.9	3.8	3.8	
Fused quartz	3.8	1.448	3.2	6.3	6.5	5-6
Mica	7.0	1.60	3.0	10	10	13.5
CaF_2	7.4	1.427	3.8	7.2	7.2	
Liquid He	1.057	1.028	5.9			
Alumina (Al_2O_3)	11.6	1.75	3.0			
Iron Oxide (Fe_3O_4)	--	1.97	3.0			
Zirconia (n-ZrO_2)	20-40	2.15	3.0			
Rutile (TiO_2)	--	2.61	3.0			
Silicon carbide	10.2	2.65	3.0			
Metals (Au, Ag, Cu)	∞	--	3-5	30-50		

Table 1.2. Hamaker constants for two media interacting across another medium (51)

Interacting Media			Hamaker constant, A (10^{-20} J)		
1	3	2	Eq. [1.20]	Exact solutions	Experiment
Air	Water	Air	3.70	3.70	
Pentane	Water	Pentane	0.28	0.34	
Octane	Water	Octane	0.36	0.41	
Dodecane	Water	Dodecane	0.44	0.50	0.5
Hexadecane	Water	Hexadecane	0.49	0.50	0.3-0.6
Water	Hydrocarbon	Water	0.3-0.5	0.34-0.54	0.3-0.9
Polystyrene	Water	Polystyrene	1.4	0.95-1.3	
Fused quartz	Water	Fused quartz	0.63	0.83	
Fused quartz	Octane	Fused quartz	0.13		
PTFE	Water	PTFE	0.29	0.33	
Mica	Water	Mica	2.0	2.0	
Alumina (Al_2O_3)	Water	Alumina	4.2	5.3	6.7
Zirconia (n-ZrO_2)	Water	Zirconia	13		
Rutile (TiO_2)	Water	Rutile	26		
Au, Ag, Cu	Water	Au, Ag, Cu	--	30-40	40 (gold)
Water	Pentane	Air	0.08	0.11	
Water	Octane	Air	0.51	0.53	
Octane	Water	Air	-0.24	-0.20	
Fused quartz	Water	Air	-0.87	-1.0	
Fused quartz	Octane	Air	-0.7		
Fused quartz	Tetradecane	Air	-0.4		-0.5
CaF_2, SrF_2	Liquid He	Vapour	-0.59	-0.59	-0.58

Table 1.3. Values of the surface tension components (in mJ /m^2) and of the viscosities (in poise) of various liquids used in direct contact angle determination, or in the capillary rise and thin layer wicking experiments (21)

Liquid	γ_L	γ_L^{LW}	γ_L^{AB}	γ_L^+	γ_L^-	η
Hexane	18.4	18.4	0	0	0	0.00326
Heptane	20.3	20.3	0	0	0	0.00409
Octane	21.6	21.6	0	0	0	0.00542
Decane	23.8	23.8	0	0	0	0.00907
Dodecane	25.35	25.35	0	0	0	0.01493
Tetradecane	26.6	26.6	0	0	0	0.0218
Cyclohexane	25.5	25.5	0	0	0	0.00912
Carbon tetrachloride	27.0	27.0	0	0	0	0.00908
Benzene	28.9	27.1	0	0	2.8	0.00604
Toluene	28.5	28.5	0	0	2.3	0.00604
Methanol	22.5	18.2	4.3	≈0.06	≈77	0.00544
Ethanol	22.4	18.8	2.6	≈0.019	≈68	0.01074
Chloroform	27.15	27.15	0	3.8	0	0.00473
cis-Decalin	32.2	32.2	0	0	0	0.0338
1-Bromonaphthalene	44.4	44.4	0	0	0	0.0489
Methylene iodide	50.8	50.8	0	0	0	0.028
Ethylene glycol	48.0	29.0	19.0	1.92	47.0	0.199
Formamide	58.0	39.0	19.0	2.28	39.6	0.0455
Glycerol	64.0	34.0	30.0	3.92	57.4	14.90
Water	72.8	21.8	51.0	25.5	25.5	0.010

Table 1.4. Surface tension components and parameters of various solid surfaces at 20 ^{o}C in mJ/m^2 (21, 26, 94-95, 97, 109)

Solid	γ_s	γ_s^{LW}	γ_s^{AB}	γ_s^{+}	γ_s^{-}
Teflon FEP	18.5	18.5	0	0	0
Polyisobutylene	25.0	25.0	0	0	0
Polypropylene	25.7	25.7	0	0	0
Corona-treated polypropylene	33.0	33.0	0	0	0
Polyethylene	33.0	33.0	0	0	0
Nylon 6,6	37.7	37.7	0	0	0
Polymethylmetacrylate (PMMA)	40.6	40.6	0	0	12.0
Polystyrene	42.0	42.0	0	0	1.1
Polyvinylalcohol	42.0	42.0	0	0	17-57
Polyvinylchloride	43.8	43.0	0.75	0.04	3.5
PEO - M.W. 6,000	43.0	43.0	0	0	64
Polyoxytetramethyleneglycol - M.W. 2,000	44.0	41.4	2.6	0.06	27.6
Co-poly(ethylene glycol, propylene glycol)-M.W. 2,000	43.0	43.0	0	0	64
Coal	39.8	39.8	0	0	2.5
Talc	41.6	37.4	4.2	2.0	2.2
Calcium Carbonate	48.0	48.0	0	0	79.0
Quartz (untreated)	191.0	76.0	115.0	--	--
Quartz (treated-DAHCl)	35.3	28.2	7.1	--	--
Silica Gel	48.8	42.0	6.8	58.4	0.2
Bentonite clay	55.5	41.2	14.3	1.5	33.3
α-Alumina	44.8	43.7	1.1	0.004	80.5
Barite	52.9	26.2	26.7	1.5	118.9

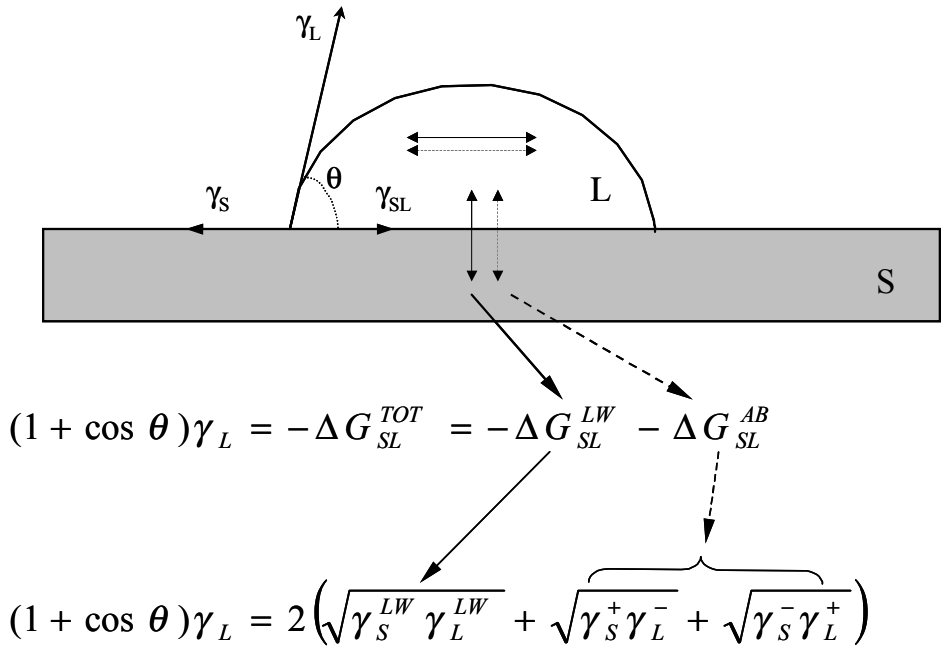

Figure 1.1. Schematic representation of the contact angle formed between a liquid droplet and a solid surface. cosθ is a measure of the equilibrium between the molecules of liquid L (horizontal arrows) and adhesion between liquid L and solid S (vertical arrows). Apolar energies are indicated by solid horizontal or vertical lines and arrows; polar (Lewis-acid base) energies are shown by dashed horizontal or vertical lines and arrows (21).

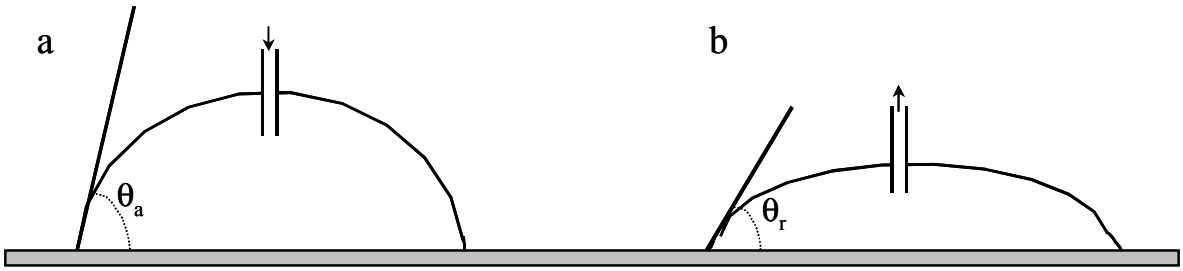

Figure 1.2. Schematic representation of (a) advancing and (b) retreating contact angles formed on a solid surface. When liquid is injected into the sessile drop the contact line advances, and when liquid is withdrawn from the drop the contact line recedes.

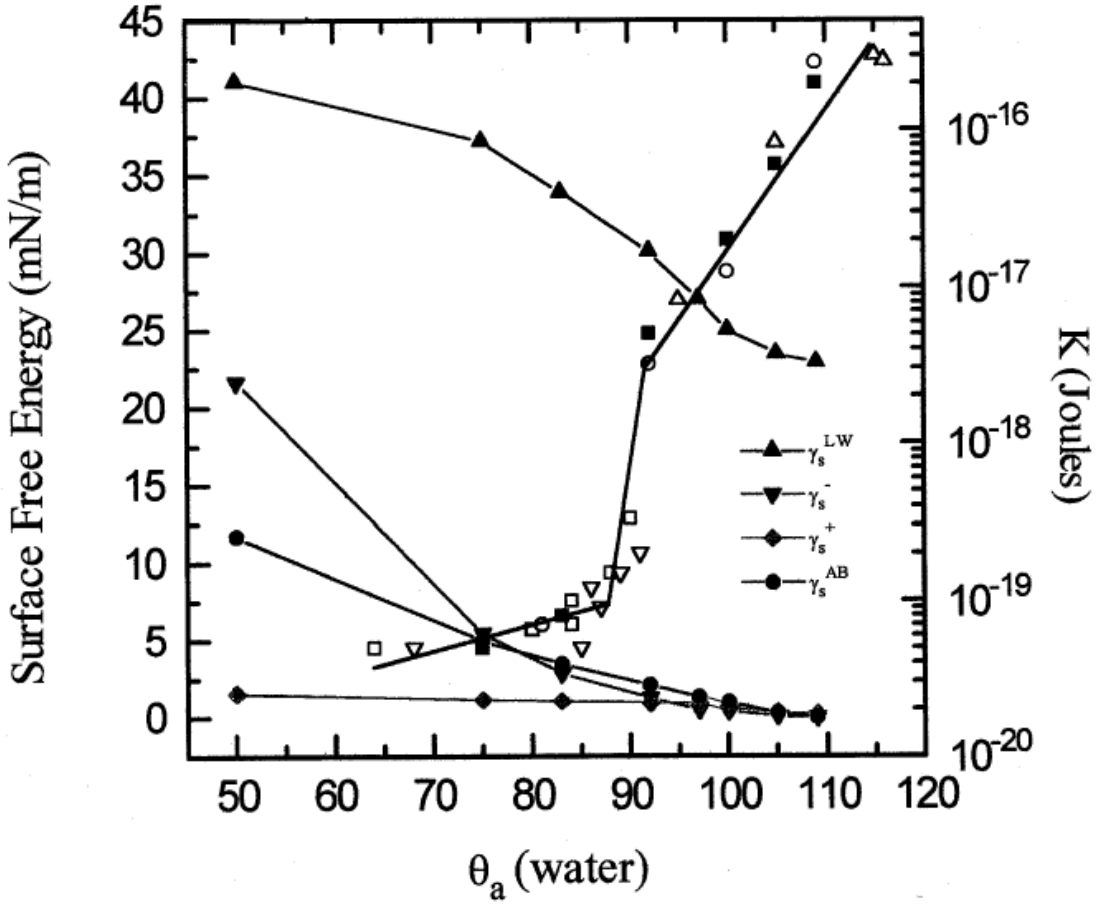

Figure 1.3. The values of hydrophobicity constant (K) and surface free energy parameters of methylated silica surfaces vs. advancing contact angle (θ_a) plot taken from the work of Pazhianur (135).